



Application of Finite Element Method for Simulation of Rock Mass Caving Processes in Block Caving Method

B. Alipenhani, H. Bakhshandeh Amnieh*, A. Majdi

School of Mining Engineering, College of Engineering, University of Tehran, Tehran, Iran

PAPER INFO

Paper history:

Received 18 August 2022

Received in revised form 19 September 2022

Accepted 22 October 2022

Keywords:

Block Caving

Numerical Modelling

Cavability

Caving Height

ABSTRACT

Determining the caving height in the block caving method requires considering a suitable caving criterion discussed in this study. The comparison between different caving criteria and choosing appropriate caving criteria for use in rock mass cavability study is the main idea of this study, which has not been investigated in previous studies. In this paper, through FEM (Finite Element Method) software, the height of the caving area in different undercutting stages was calculated using the criteria of displacement and shear and tensile failure. The results revealed that when using shear and tensile failure, the height of the caving was almost four times higher than the displacement criterion. The height of the caving reaches 249.15 m in this case. However, it is 59 and 107 m considering the allowable displacement and strain criteria, respectively. According to empirical methods, the caving propagated to the highest block height. Thus, the shear and tensile failure criteria predict the caving height better than the displacement criteria.

doi: 10.5829/IJE.2023.36.01a.16

NOMENCLATURE

MRMR	Mining Rock Mass Rating	GSI	Geological strength index	S_1	Maximum principal stress
CPF	Caving Propagation Factor	ϵ_{all}	Allowed strain	S_3	Minimum principal stress
FEM	Finite Element Method	ϵ_u	Critical strain	m_b	Hoek Brown Constant
σ_c , UCS,	Uniaxial Compressive Strength	U_{max}	Maximum Displacement	s	
LTCC	Longwall Top Coal Caving	RES	rock engineering system	SRM	Syntetic Rock Mass

1. INTRODUCTION

In open pit mines, the ore is extracted from different blocks and benches [1]. There is a possibility of high production. Block caving is the best method to exploit deep mass deposits, competing with open-pit mining [2]. There is some large deposit that extends from the surface to deep underground. Such deposits should be extracted by combining open pit and underground mining methods [3]. In these cases, Block caving is an appropriate option [2].

In the large-scale caving method, it is essential to cave the ore and rock columns [4]. In addition to empirical methods, numerical modelling is used to determine the rock mass cavability. Numerical methods are extensively used in solving stress-deformation boundary value problems related to mining geomechanics. Analytical

methods cannot solve these problems. The problems occur when it is impossible to describe the boundary conditions, such as problem geometry with simple mathematical functions, partial differential equations being nonlinear, the problem space being heterogeneous, or the equations comprising the corresponding rock mass being nonlinear. Such conditions are primarily present in caving analyzes associated with nonlinear definitions and rock mass behaviour [4].

According to Brown [4], reviewing caving mines, numerical modelling provides a more accurate mathematical and fundamental understanding of caving initiation and propagation than empirical (or analytical) methods.

Rock masses are assumed to have continuous behaviour in continuum numerical models since rock mass behaviour is not controlled kinematically by

*Corresponding Author Institutional Email: hbakhshandeh@ut.ac.ir
(H. Bakhshandeh Amnieh)

discontinuities. The rock mass characteristics are defined as equivalent, i.e., a combination of intact rock and joints. Also, the response of materials is assumed to be described by the theories of elasticity and plasticity, which are expressed as flexible deformation and plastic yield [5].

In general, the methods used for assessing the rock mass cavability and propagation of caving are divided into three categories: analytical, empirical, and numerical. Tables 1 and 2 show the history of the performed studies in this field.

In past research, different caving criteria were not considered, as shown in Tables 1 and 2. Another issue that has not been investigated in past studies is the height of caving according to different criteria. These two issues are discussed in this paper.

The finite element method is common in solving the problems of tunnels and underground spaces [6, 7]. This paper uses this method to analyze the caving behaviour of the rock mass in the block caving method.

It is essential to choose the rock mass caving criterion to investigate its cavability in the block caving method. The main idea of this paper is to determine the appropriate criteria for rock mass caving. To date, no study has been presented that compares different criteria of displacement, shear and tensile failure, and strain in the rock mass caving in the block caving method. In the present paper, the caving behaviour of the rock mass was evaluated using displacement criteria, shear and tensile failure and strain. On the real scale, numerical modelling on stepwise propagation of undercutting, deformation, induced stresses, and height of caving was calculated and compared.

2. RESEARCH METHODOLOGY

The rock mass parameters inserted in the software are critical to achieve a reliable output in modelling with FEM. In a numerical model, the physical and mechanical properties of the rock mass are obtained from the detailed design report of the Iron cap mine [8]. Iron Cap deposit, part of the KSM property located in the Coast Mountains of northwestern British Columbia. The location, dimensions, and dip of the mineralized material at Iron Cap indicated that it was suitable for block caving.

The rock mass characteristics have been obtained using Rock Data software based on the characteristics of intact rock and discontinuities and fractures (including faults and cracks). Therefore, the effect of the geological strength index (GSI) was indirectly investigated. In other words, by entering the value of the geological strength index in the Rock Data software, the output of this software, which is the characteristics of the rock mass, has been used as the input of the FEM software.

The cavability assessments made using Laubscher's and Mathews' methods indicate that the size (diameter) of the footprint required to initiate and propagate caving is approximately 100 m [8]. For better representation, the properties of the rock mass entered in the modelling are presented in Table 3. In this table, UCS shows the uniaxial compressive strength of intact rock, and GSI shows the geological strength index. The undercutting operation is modelled in a 2D finite element environment. Then, the height of the caving is measured considering the two criteria of displacement and shear and tensile failure. Also, Sakurai's critical strain criterion [9] was investigated. The amount of allowed strain was calculated according to the relations provided by Sakurai [10], representing the allowed strain at each step of undercutting and displacement followed by excavation (Equations (1) and (2)). Finally, a suitable criterion is proposed to estimate the caving height in the block caving method.

$$\varepsilon_{all} = \frac{\sigma_c}{E}, \quad (1)$$

$$\varepsilon_u = \frac{U_{max}}{Span} \quad (2)$$

In order to validate the modelling results, Laubscher and Flores' models were used. These two methods are explained below.

2. 1. Laubscher Caving Chart In 1990, Laubscher developed the most commonly used method to estimate cavability based on a combination of data from large mines in South Africa. Laubscher's caving chart illustrates the three possible modes as follows [11]:

- No caving (stable);
- Transition status: It is a situation in which caving begins, but its propagation is low.
- Caving: It is a condition in which continuous caving occurs.

Using this chart and determining the mining rock mass rating (MRMR) and the hydraulic radius of the deposit footprint, the status of the rock mass can be determined (Figure 1).

2. 2. Flores's Coefficient Flores and Karzulovic [15] proposed a propagation coefficient (CPF) for caving to determine whether the caving is probable, transition, or spontaneous, which is very similar to the transition and stable areas of Laubscher. CPF was defined as the ratio between the difference of the principal stresses in the caving area and the maximum difference of the stresses that the rock mass can withstand (Equation (3)).

$$CPF = \frac{S_1 - S_3}{S_{1Max} - S_3} = \frac{S_1 - S_3}{\sigma_c (m_b \frac{S_2 + S_3}{\sigma_{ci}})^a} \quad (3)$$

TABLE 1. History of continuous numerical modelling used for rock mass caving assessment.

References	Purpose and application	Disadvantage
Palama and Agarwal [12]	Numerical modelling of caving progress at the El Teniente mine	The assumption of the environment's elasticity in modelling could not explain the mechanism of stress caving. They are not considering different criteria for caving.
Barla et al. [13]	2D finite element simulation at the Grace Mine in Pennsylvania, USA	This model revealed the limitations of the elastic modelling performed by Palama and Agarwal. They are not considering different criteria for caving.
Rech and Loring [14]	Reproduction of caving conditions at the Henderson mine in Colorado, USA	Lack of modelling the caving propagation and not calculating the height of caving
Singh et al. [15]	Study of caving at the Rajpura Dariba mine using FLAC software	The assumption of elasticity of the environment in modelling They are not considering different criteria for caving.
Lorig [16]	Caving simulation in axial-symmetric models considering cylindrical undercut and lithostatic stress	The difference between the shape of caving in the numerical model and real cases They are not considering different criteria for caving.
Trueman et al. [17]	Determining the amount of stresses in production and undercut production tunnels in some block and panel caving mines as well as the required support system	Lack of modelling of the caving process
Brown [4]	Investigation of the effects of depth, stress, large-scale discontinuities, rock mass strength, and groundwater on the cavability by determining the caving propagation factor (CPF)	The assumption of vertical caving propagation and homogeneous rock mass properties can be considered as the limitations of the practicality of this method (CPF method). They are not considering different criteria for caving.
Yasitli and Unver [18]	Evaluation of the abutment pressure around the face and the type of the material flow into the stope	They aimed to investigate the stress concentration surrounding the undercut face and the type of material flow into the stope.
Pierce et al. [19]	3D Simulation of caving behavior at the Northparkes mine	They are not considering different criteria for caving. They are not calculating the height of the caving.
Beck et al. [20]	Evaluation of the caving propagation behavior in nickel and diamond deposits using Abaqus	They are not considering different criteria for caving. They are not calculating the height of the caving.
Gauri Shankar et al. [21]	Investigation of the effects of mining depth, extraction height, horizontal stresses, immediate roof thickness, immediate roof strength, main roof thickness, and main roof strength on the caving behavior	They are not considering different criteria for caving. They are not calculating the height of the caving.
Woo et al. [22]	Evaluation of subsidence at the Palabora mine using FLAC3D	Lack of modelling of the caving process They are not calculating the height of the caving.
Sainsbury [5]	Studying the caving propagation and subsidence	They are not considering different criteria for caving and using displacement alone. They are not calculating the height of the caving.
Potvin et al. [23]	Centrifuge modelling of caving mechanism using 3DEC and FLAC3D	They are not considering different criteria for caving. Small-scale modelling of caving differs significantly from real-scale results.
Öge et al. [24]	Prediction of cavability in the Top Coal method using the empirical and numerical methods	They are assuming displacement criteria for caving alone. They are not calculating the height of the caving.
Xia et al. [25]	Investigation of the mechanism of ground pressure damage caused by poor undercutting using FLAC3D	They are not calculating the height of the caving. They are not considering different criteria for caving. Lack of modelling of the caving process
Xia et al. [26]	Investigation of the mechanism of ground pressure damage process on the extraction opening during deposit extraction by FLAC3D	They are not calculating the height of the caving. They are not considering different criteria for caving.

TABLE 2. History of analytical, Distinct element numerical modelling, physical and other methods used for rock mass caving assessment

Model type	References	Purpose and application	Disadvantage
Analytical	Someehneshtin et al.) [27]	Determination of the optimal block size in the block caving method by the analytical method	They are not considering different criteria for caving and using shear strength alone. They are not calculating the height of the caving.
	Gao et al. [28]	Modelling of progressive caving of layers on top of coal mining panel by the long wall method using UDEC	They are not considering different criteria for caving and using displacement alone. They are not calculating the height of the caving.
	Rafiee et al. [11]	Investigating the effect of 7 different parameters on cavability using the SRM technique	They are not calculating the height of the caving. They are not considering different criteria for caving and using displacement alone.
	Song et al. [29]	Numerical modelling based on 3D particles for process simulation (LTCC)	Modelling the discharge process in the LTCC method and not modelling the process of creating an undercut and caving initiations and propagation
Numerical Modelling	Mohammadi et al. [30]	Evaluating the cavability of the immediate roof and estimating the caving span in the long wall method	They are not calculating the height of the caving. They are not considering different criteria for caving and using displacement alone.
	Wang et al. [31]	Investigating the effect of top coal block size on the caving mechanism	They are not calculating the height of the caving. They are not considering different criteria for caving
	Alipenhani et al. [32]	Determination of caving hydraulic radius of rock mass in the block caving method using numerical modelling and multivariate regression	They are not considering different criteria for caving and using displacement alone.
	Alipenhani et al. [33]	Cavability Assessment of Rock Mass in Block Caving Mining Method based on Numerical Simulation and Response Surface Methodology	They are not considering different criteria for caving and using displacement alone.
Physical modelling	Jacobsz and Kearsley [34]	In a centrifuge experiment, the results of placing a weak mass of artificial rock under high and low horizontal stress conditions were examined.	Lack of modelling of the caving process
	Bai et al. [35]	In this study, experiments were performed on two large-scale physical models including sand, gravel, gypsum, and mica to investigate the cavability of top coal with hard rock bands based on two real cases.	They are not calculating the height of the caving. They are not considering different criteria for caving.
	Khosravi et al. [36]	Investigation of caving mechanism in the block caving method using physical modelling	They are not calculating the height of the caving. They are not considering different criteria for caving Small-scale modelling of caving that differs greatly from real-scale results
	Alipenhani et al. [37]	Physical model simulation of block caving in jointed rock mass	Lack of modelling of the caving process in continuum mode
Fuzzy rock engineering system	Rafiee et al. [10]	Investigation of the effective factors on cavability using fuzzy system	They are not calculating the height of the caving. They are not considering different criteria for caving
RES	Rafiee et al. [38]	Investigation of the factors affecting cavability using rock engineering system (RES)	They are not calculating the height of the caving. They are not considering different criteria for caving
Probabilistic	Mohammadi et al. [30]	Presenting a probabilistic model for estimating the minimum caving span in the long wall method	They are not calculating the height of the caving. They are not considering different criteria for caving

TABLE 3. Input material parameters are used in numerical modelling [40].

Parameter	UCS (intact rock)	GSI	mi	D	Hoek Brown Criterion			Mohr-Coulomb		Rock Mass Parameters		
					mb	s	a	C	φ	σ_t	σ_{cm}	E_m
Unit	MPa	-	-	-	-	-	-	MPa	°	MPa	MPa	GPa
Value	102	65	20	1	2.49	0.0049	0.501	5.18	35.42	0.2	21.9	14.22

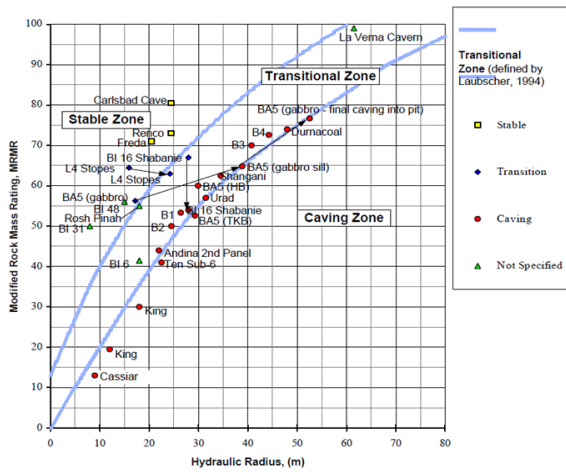


Figure 1. Laubscher caving chart [2]

where S_1 (maximum principal stress) and S_3 (minimum principal stress) are known from the results of the numerical models, σ_c is the uniaxial compressive strength of the intact rock, and m_b , s and a are material constants that depend on the value of m_i and the geological strength index of the rock mass, GSI.

The schematic flowchart of the methodology is depicted in Figure 2.

3. NUMERICAL MODELLING

3.1. Development of the Numerical Model Two-dimensional modelling facilitates entering more details considering the computer capacity available in the model. The model geometry and geomechanical properties used in the modelling were selected based on Iron cap mine data. Based on the typical values mentioned in the international caving study, the width and height of the

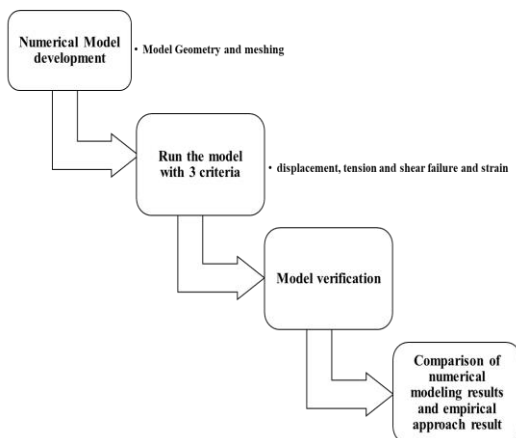


Figure 2. Schematic flowchart of the methodology

undercutting were 100 and 8 m, respectively [6]. The boundary dimensions were 500 m in the horizontal direction (from the edge of the section) and 500 m in the vertical direction. A mesh sensitivity study was conducted on the dimensions (Figure 3). The mesh density was 1500 based on a sensitivity analysis. Figure 4 represents the results of vertical displacement in the center of the undercutting roof for different dimensions of the model boundary distance. The results are considered for the case where the undercut is fully excavated (100 m). Based on the height of the ore block (400 m) in the Iron cap mine and the possibility of displaying the height of the caving area, the whole ore column was modelled. Eight-node elements with four integration points were used to increase the accuracy of the modelling results. Numerical modelling was performed in a continuous environment. Figure 5 represents the model geometry. As seen, the undercutting is excavated in ten steps. The modelling consists of eleven steps, the first of which is to balance the model and the next steps are sequential digging the undercutting.

The shape of the yield zone, the amount of displacement, and the stress changes were measured at different stages of undercutting propagation. After constructing the numerical model and applying the boundary conditions, the model was implemented until equilibrium was reached. Then, the undercutting operation was conducted from the left in steps of 10 m (Figure 5). In caving mines, the undercut excavation steps are usually 10 meters. Accordingly, in the numerical model, the excavation step in each stage is 10 meters. To release the stress and permit the ore to collapse properly, the time steps about 30 minutes were undertaken (in each step). At each stage, displacement and stress values were recorded. In the initial stage, boundary conditions were applied, and the Mohr-Coulomb failure criterion was considered for the materials.

In the numerical model, Mohr-Coulomb behavioural model was used. The model was first balanced with elastic behaviour based on the modelling process. Then, the behavioural model of the rock mass was changed to Mohr-Coulomb, and a undercut was created. The sides of the model were limited in the horizontal direction, and the lower part of the model was limited in the horizontal and vertical directions.

4. RESULTS ANALYSIS AND DISCUSSION

Figures 5 and 6 represent the displacement and failure changes at different undercutting stages described in the following lines.

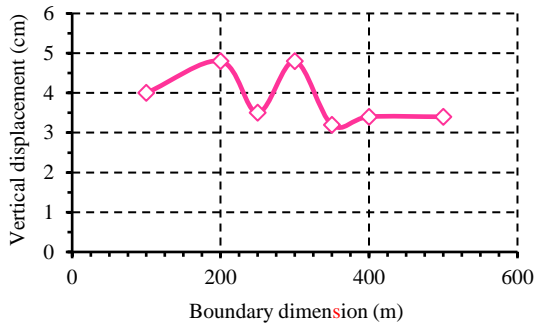


Figure 3. The effect of different boundary distances on modelling results

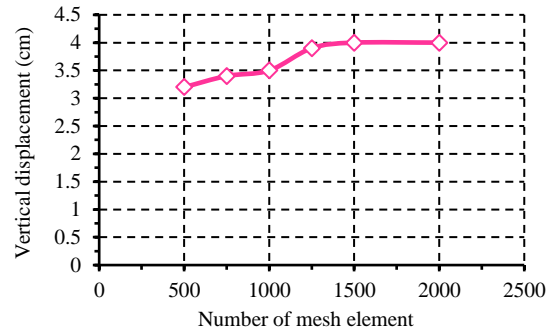


Figure 4. The displacement of the undercutting roof in different dimensions of the element

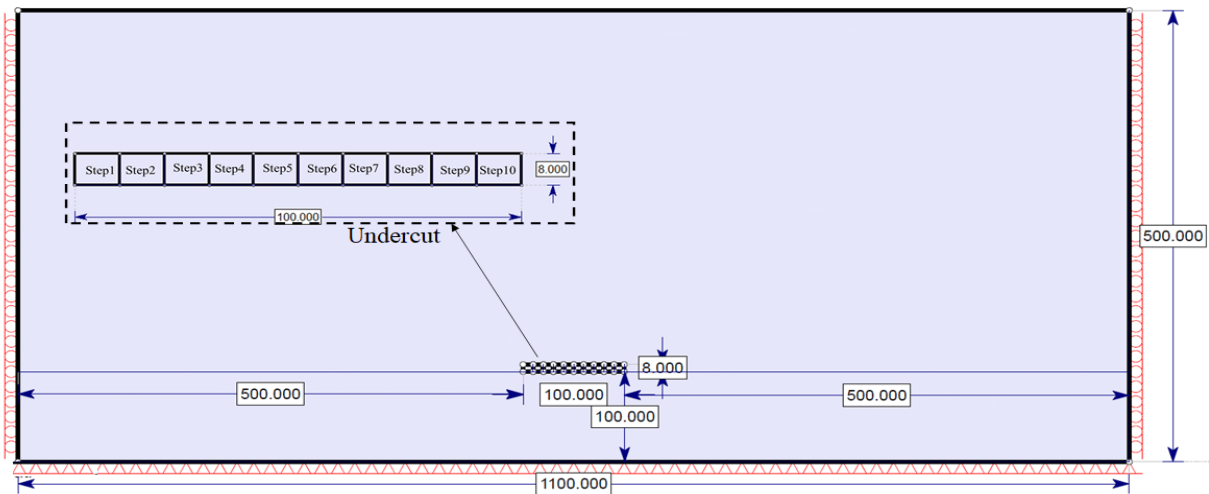


Figure 5. Model geometry and boundary condition

4. 1. Displacement Changes Around the Undercut

As it is known, by undercutting operations, the rock mass above the undercutting loses its support and undergoes deformation and failure. In stage 1, where undercutting progresses 10 m, a very small deformation of a few millimetres is observed in the rock mass (Figure 6). Therefore, no failure or caving occurs, and the rock mass remains unchanged at this stage. However, by progressing the undercutting, the maximum amount of stress was created, thus increasing the displacements. According to Sainsbury [5], a displacement of 1 m indicates the caving. Accordingly, in the seventh stage (undercutting width of 70 m), caving initiates. Accordingly, the height of the caved area is 3.44 m. Figure 7 represents the maximum displacement at each stage. As seen, when the undercutting progresses, the amount of displacements increases. The slope of these changes highly increased from the span of 60 m onwards. Up to the 70-meter span, the amount of displacement is less than 1 meter, which indicates that the caving has not been initiated.

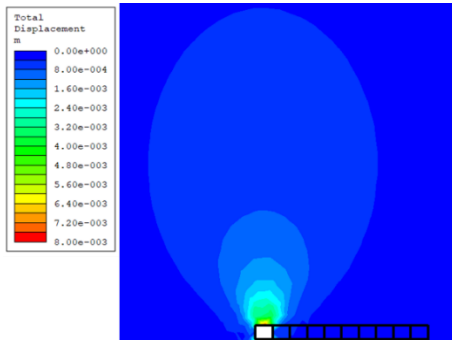
As a result of undercutting, stresses are redistributed

around the undercut. The stress concentration increases on both sides of the undercut. As the undercutting progresses, the de-stressed zone height and stress concentration increase. When the value of this stress concentration reaches a certain level, the materials of the undercut’s roof begin to fail and move (Figures 6 and 7).

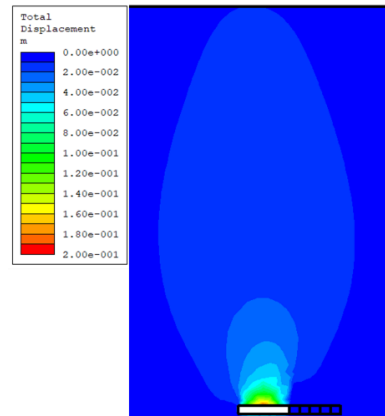
As shown in Figure 6, the caving area is an ellipsoid with a vertical extension. This area is the motion ellipsoid, and the regions with less displacement are called active ellipsoids.

Figure 8 represents the changes in the caved area's height at different undercutting stages. In the 70-meter span where caving occurred, the caving height is limited. As the span increases, the caving height increases up to 60 meters (in a 100-meter span).

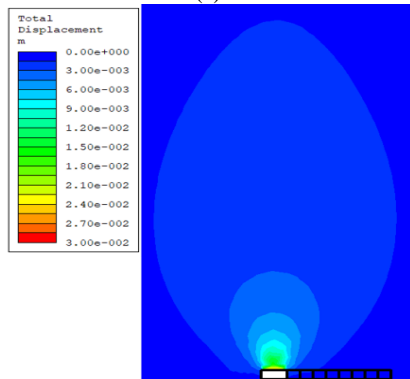
The ratio of the caving height to the span width increases with the increase in the width of the span. This ratio reaches 0.6 at the maximum span (100m), indicating insufficient span width. However, in a mining operation, the span width of 100 meters is enough to cave the entire ore column. This indicates the inappropriateness of displacement criteria for caving.



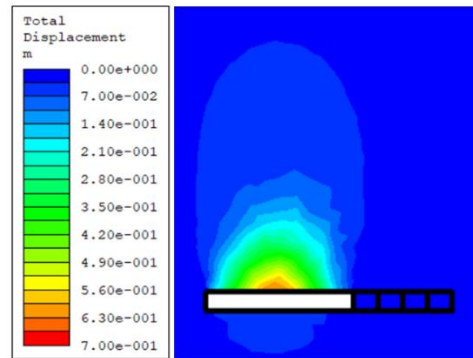
(a)



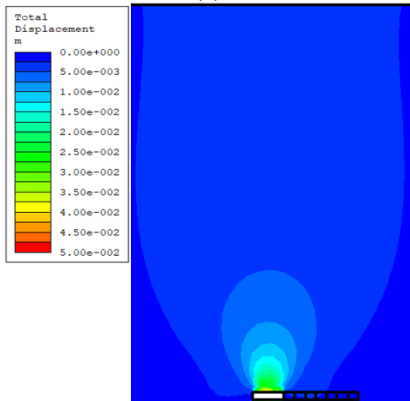
(e)



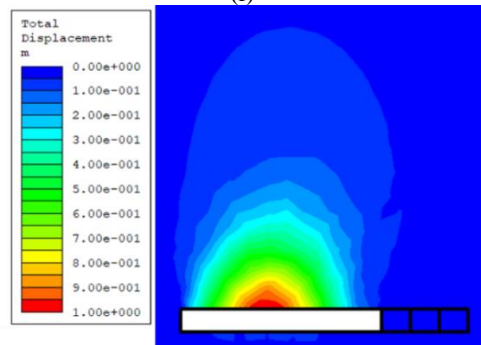
(b)



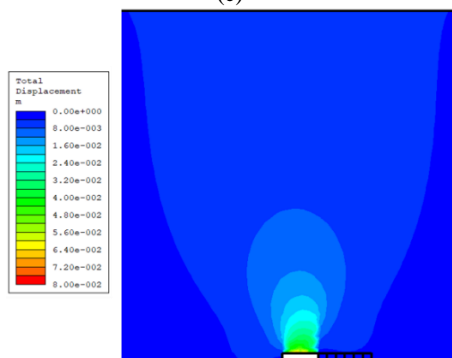
(f)



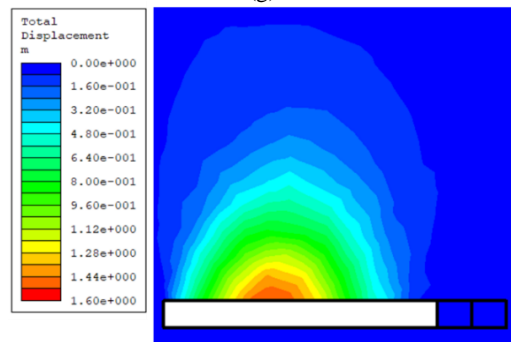
(c)



(g)



(d)



(h)

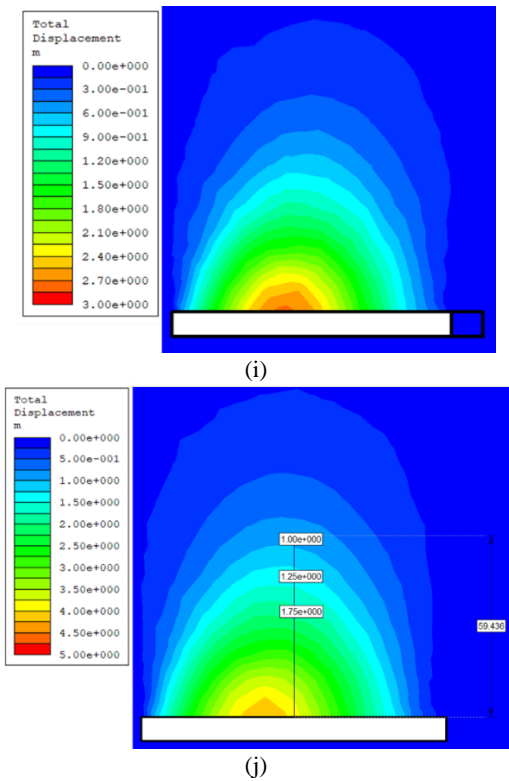


Figure 6. Contours of vertical displacement in different sequence :a) stage 1 (span = 10m) b) stage 2 (span = 20m), c) stage 3 (span = 30m), d) stage 4 (span = 40m), e) stage 5 (span = 50m), f) stage 6 (span = 60m). g) stage 7 (span = 70m), h) stage 8 (span = 80m), i) stage 9 (span = 90m), j) stage 10 (span = 100m)

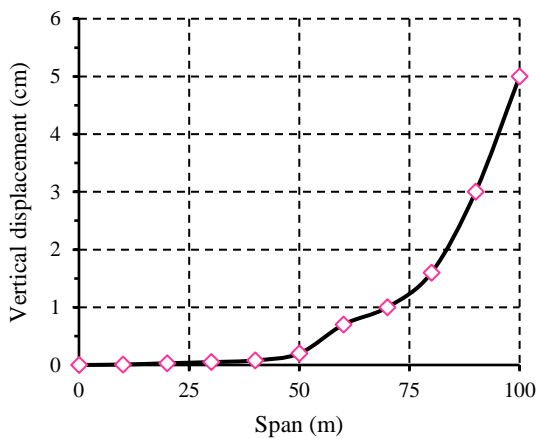


Figure 7. Vertical displacement in undercutting stages

4. 2. Changes in Areas with Failure Around Undercutting

As stated in section 4.1, in the case using the 1-meter displacement as the caving criterion, the caving initiate from the 70-meter span. However, in

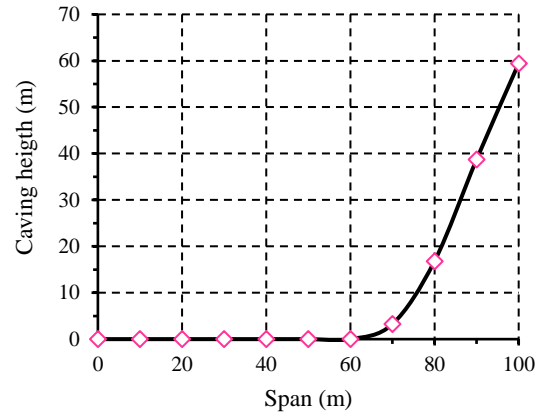


Figure 8. Caving height in undercutting stages

the case of using the shear and tensile failure criterion, in the second stage (undercut span of 20 m), some elements experienced tensile, and shear failure and the caving initiate (Figure 9). At this stage, the height of the caved area is 9.51 m. Thus, a shear failure was created. Furthermore, the shape of the caved area is different in the two cases. Likewise, as the undercutting progresses 30 m, the yielded areas increase and widen, thus propagating the caving.

The numerical modelling results confirm that a conceptual model of a self-sustained propagating cave was developed by Duplancic and Brady [38], as shown in Figure 10.

The intact zone at the upper side of the caving zone in the numerical model is the elastic region in Dupancic conceptual model.

Figure 11 shows the results of measuring the height of the caving area based on the shear failure criterion. Figure 12 also shows a diagram based on the results obtained from both criteria and the plastic strain criterion.

As evident in Figure 12, the ratio of the height of the caving zone to the span in the case of considering the criterion of tensile shear failure is higher than in the other two cases (twice as much on average).

The strain contour corresponding to the 100-meter span is shown in Figure 13. As it is known, the caving height obtained from this criterion is higher than the displacement criterion and lower than the tensile failure criterion. It can be said that the strain criterion is more suitable than the displacement criterion to determine the height of the caving.

According to the results, the height of the caving area in the shear and tensile failure criterion is much higher than the displacement criterion. The height of the caving obtained from the strain criterion is within the values obtained from the other two methods.

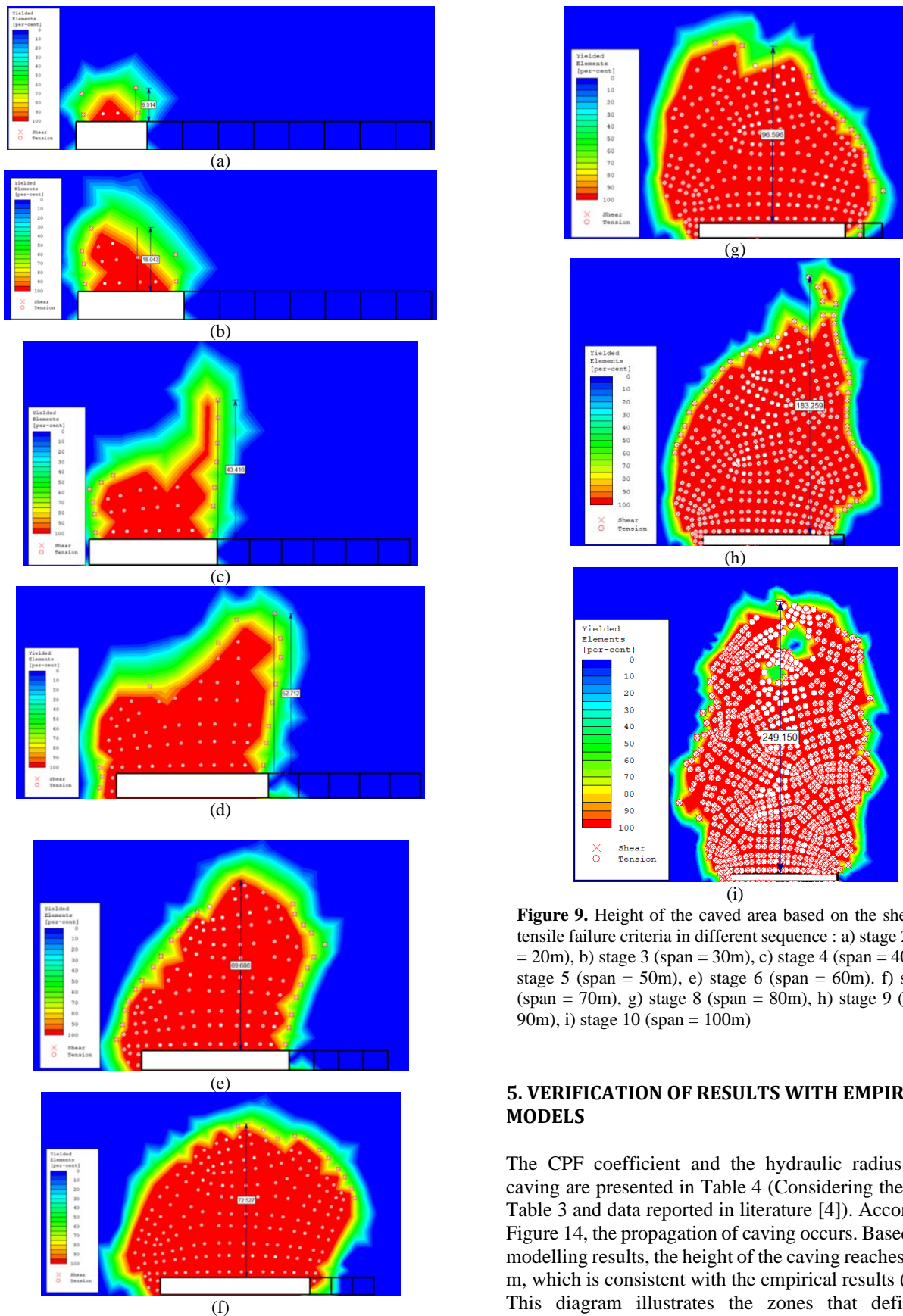


Figure 9. Height of the caved area based on the shear and tensile failure criteria in different sequence : a) stage 2 (span = 20m), b) stage 3 (span = 30m), c) stage 4 (span = 40m), d) stage 5 (span = 50m), e) stage 6 (span = 60m). f) stage 7 (span = 70m), g) stage 8 (span = 80m), h) stage 9 (span = 90m), i) stage 10 (span = 100m)

5. VERIFICATION OF RESULTS WITH EMPIRICAL MODELS

The CPF coefficient and the hydraulic radius of the caving are presented in Table 4 (Considering the data in Table 3 and data reported in literature [4]). According to Figure 14, the propagation of caving occurs. Based on the modelling results, the height of the caving reaches 249.15 m, which is consistent with the empirical results (220m). This diagram illustrates the zones that define the

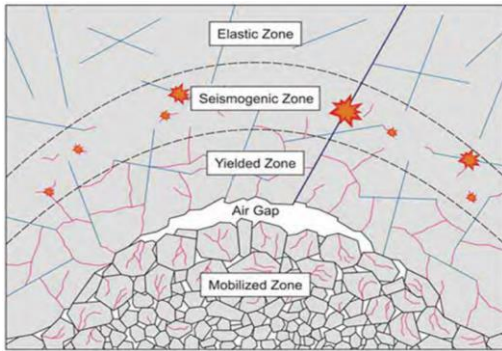


Figure 10. Conceptual diagram showing the main behavioural regions of a propagating cave based on underground observations and instrumentation [5]

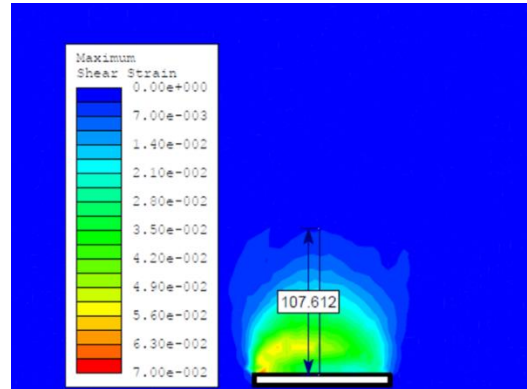


Figure 13. The strain contour around undercut (span = 100 m)

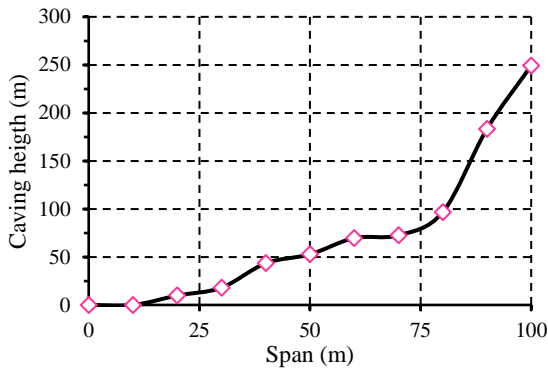


Figure 11. Height of the caved area in different undercutting stages based on the shear and tensile failure criteria

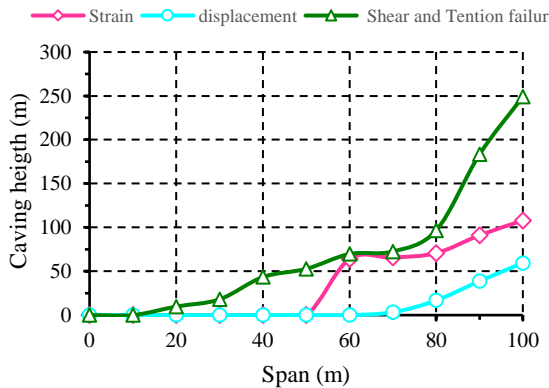


Figure 12. The changes in the height of the caved area in different undercutting stages based on different criteria

likelihood of caving propagation in terms of the Caving Propagation Factor. The h/B ratio can be calculated by calculating the CPF.

Moreover, according to the Laubscher diagram, a hydraulic radius of 25 m (100 by 100 m) is enough to start and propagate the caving, which is close to the modelling results.

TABLE 4. Determination of caving hydraulic radius based MRMR and presented equation

Factor	Calculated values	rate
Rock block rate	$RBS = 0.8 \times IRS = 0.8 \times 102 = 81.6$	10
joint spacing	2.8m	22
RQD	93%	14
Joint condition	Large scale: Moist, straight, small scale: Moist, rough undulating, No alteration and no filling, $C=0$ and $\varphi = 30$ ($40 \times 0.7 \times 0.75 = 27$)	21
Orientation adjustment	3 joints, 2 inclined (60 degree)	0.8
Water adjustment	An environment without water is considered.	1
Blasting adjustment	None	1
Weathering adjustment	None	1
induced stresses adjustment	Depth of 600 meters	0.9
Sum of rates	82	
MRMR	$67 \times 0.8 \times 0.9 = 48.24$	48
Caving hydraulic radius from Laubscher chart	25 m	
Span (B)	100 m	
CPF	1.13	
h/B	2.2	
H (m)	$2.2 \times 100 = 220$	

RBS = Rock block strength, IRs = Intuit rock strength

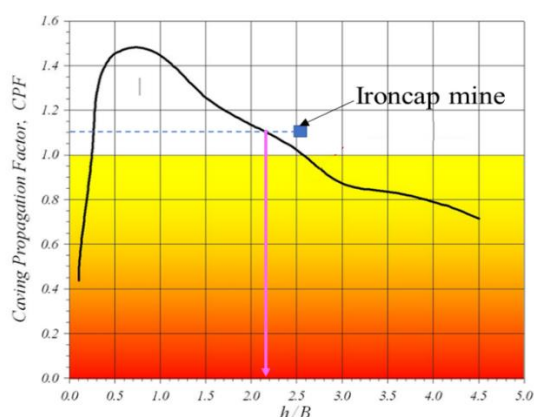


Figure 14. The propagation status of Iron cap mine caving using CPF

6. CONCLUSION

Block caving has a high production capacity and can be compared with the open pit method regarding operational costs and production rate.

For realistic numerical modelling of the caving mechanism in the block caving method, stresses in the cave back, the displacements, tensile and shear failure, and strain, two-dimensional numerical modelling has been used in FEM software. In addition, the input parameters of the numerical model were obtained from the design report of Iron Cap Deposits.

The caving of the rock mass using displacement criteria, shear, tensile failure, and strain initiated at the span width of 70 meters, 20 meters, and 60 meters, respectively. However, the caving propagations in these spans do not propagate to the top level of the ore block. In order to continue the caving up to the height of the ore block, the span was increased to 100 meters. In this span, the shear and tensile failure criteria have closer results to the actual case than the other two criteria. According to the modelling results, the maximum height of the caving area is obtained using the shear and tensile failure criteria. The height of the caving reaches 249.15 m in this case. However, it is 59 and 107 m considering the allowable displacement and strain criteria, respectively. The predicted caving height using the tensile failure criterion is closer to the empirical results. Moreover, the shape of the caving zone is closer to the shape of the cave back observed in caving mines when using shear and tensile failure criteria.

Using the data of the Iron Cap mine, the value of MRMR 48 is obtained, which is obtained by placing it in the Laubscher chart and using the caving propagation factor. The value of the caving height is 220 meters.

The obtained results largely confirm the general results of previous studies, which shows the reliability of this modelling and its results.

5. REFERENCES

- Rahmanpour, M. and Osanloo, M., "Resilient decision making in open pit short-term production planning in presence of geologic uncertainty", *International Journal of Engineering, Transactions A: Basics*, Vol. 29, No. 7, (2016), 1022-1028. doi: 10.5829/idosi.ije.2016.29.07a.18.
- Laubscher, D.H., "Cave mining handbook", *De Beers, Johannesburg*, Vol., No., (2003), 138.
- Soltani Khaboushan, A. and Osanloo, M., "An uncertainty-based transition from open pit to underground mining", *International Journal of Engineering, Transactions A: Basics*, Vol. 32, No. 8, (2019), 1218-1224. doi: 10.5829/ije.2019.32.08b.19.
- Brown, E.T., "Block caving geomechanics", (2002).
- Sainsbury, B., "A model for cave propagation and subsidence assessment in jointed rock masses", University of South Wales, (2012).
- Hematian, J., "Appropriate loading techniques in finite element analysis of underground structures", *International Journal of Engineering, Transactions A: Basics*, Vol. 11, No. 1, (1998), 43-52.
- Ali, D., Abbas, H. and Abdullah, T., "Numerical analysis of stress distribution during tunneling in clay stone rock", *International Journal of Engineering, Transactions A: Basics*, Vol. 33, No. 8, (2020), 1472-1478. doi: 10.5829/IJE.2020.33.08B.05.
- Smolik, J., *Pre-feasibility block cave mine design - iron cap deposit*. 2012: Vancouver: Seabridge Gold Inc.
- Sakurai, S., "Lessons learned from field measurements in tunnelling", *Tunnelling and underground space technology*, Vol. 12, No. 4, (1997), 453-460. doi: 10.1016/S0886-7798(98)00004-2.
- Rafiee, R., Ataei, M., KhalooKakaie, R., Jalali, S.E. and Sereshki, F., "A fuzzy rock engineering system to assess rock mass cavability in block caving mines", *Neural Computing and Applications*, Vol. 27, No. 7, (2016), 2083-2094. doi: 10.22059/IJMG.2022.339663.594953
- Rafiee, R., Ataei, M., KhalooKakaie, R., Jalali, S., Sereshki, F. and Noroozi, M., "Numerical modeling of influence parameters in cavability of rock mass in block caving mines", *International Journal of Rock Mechanics and Mining Sciences*, Vol. 105, (2018), 22-27. <https://doi.org/10.1016/j.ijrmmms.2018.03.001>
- Palma, R. and Agarwal, R., *A study of the cavability of primary ore at the el teniente mine*. 1973, Technical Report from Colombia University, New York.(niepublikowane).
- Barla, G., Boshkov, S. and Pariseau, W., "Numerical modeling of block caving at the grace mine", *Geomechanics Applications in Underground Hardrock Mining, Turyn, Wlochy*, (1980), 241-256.
- Rech, W. and Lorig, L., "Predictive numerical stress analysis of panel caving at the henderson mine", *Proc. of MASSMIN*, Vol. 92, (1992), 55-62.
- Singh, U., Stephansson, O. and Herdocia, A., "Simulation of progressive failure in hanging-wall and footwall for mining with sub-level caving", *Transactions of the Institution of Mining and Metallurgy Section A-Mining Industry*, Vol. 102, (1993), A188-A194.
- Lorig, L., "The role of numerical modelling in assessing caveability", Itasca Consulting Group Inc., Report to the International Caving Study, ICG00-099-3-16, (2000).
- Trueman, R., Pierce, M. and Wattimena, R., "Quantifying stresses and support requirements in the undercut and production level drifts of block and panel caving mines", *International Journal of Rock Mechanics and Mining Sciences*, Vol. 39, No. 5, (2002), 617-632. [https://doi.org/10.1016/S1365-1609\(02\)00060-6](https://doi.org/10.1016/S1365-1609(02)00060-6)

18. Yasitli, N. and Unver, B., "3d numerical modeling of longwall mining with top-coal caving", *International Journal of Rock Mechanics and Mining Sciences*, Vol. 42, No. 2, (2005), 219-235.
19. Pierce, M., Young, P., Reyes-Montes, J. and Pettitt, W., *Six monthly technical report, caving mechanics, sub-project no. 4.2: Research and methodology improvement and sub-project 4.3, case study application. Itasca consulting group, inc., report to mass mining technology project, 2004-2007*. 2006, ICG06-2292-1-Tasks 2-3-14, March.
20. Beck, D., Reusch, F. and Arndt, S., "Estimating the probability of mining-induced seismic events using mine-scale, inelastic numerical models", in *Deep Mining 2007: Proceedings of the Fourth International Seminar on Deep and High Stress Mining*, Australian Centre for Geomechanics., (2007), 31-41.
21. Singh, G.S.P. and Singh, U.K., "Numerical modeling study of the effect of some critical parameters on caving behavior of strata and support performance in a longwall working", *Rock Mechanics and Rock Engineering*, Vol. 43, No. 4, (2010), 475-489. <https://doi.org/10.1007/s00603-009-0061-1>
22. Woo, K.-S., Eberhardt, E., Rabus, B., Stead, D. and Vyazmensky, A., "Integration of field characterisation, mine production and insar monitoring data to constrain and calibrate 3-d numerical modelling of block caving-induced subsidence", *International Journal of Rock Mechanics and Mining Sciences*, Vol. 53, (2012), 166-178. <https://doi.org/10.1016/j.ijrmms.2012.05.008>
23. Cumming-Potvin, D., Wesseloo, J., Pierce, M., Garza-Cruz, T., Bouzeran, L., Jacobsz, S. and Kearsley, E., "Numerical simulations of a centrifuge model of caving", in *Caving 2018: Proceedings of the Fourth International Symposium on Block and Sublevel Caving*, Australian Centre for Geomechanics., (2018), 191-206.
24. Öge, İ.F., "Prediction of top coal cavability character of a deep coal mine by empirical and numerical methods", *Journal of Mining Science*, Vol. 54, No. 5, (2018), 793-803. <https://doi.org/10.1134/S1062739118054903>
25. Xia, Z., Tan, Z., Pei, Q. and Wang, J., "Ground pressure damage evolution mechanism of extraction level excavations induced by poor undercutting in block caving method", *Geotechnical and Geological Engineering*, Vol. 37, No. 5, (2019), 4461-4472. <https://doi.org/10.1007/s10706-020-01264-y>
26. Xia, Z., Tan, Z. and Miao, Y., "Damage evolution mechanism of extraction structure during mining gently dipped orebody by block caving method", *Geotechnical and Geological Engineering*, Vol. 38, No. 4, (2020), 3891-3902. <https://doi.org/10.1007/s10706-020-01264-y>
27. Somehneshin, J., Oraee-Mirzamani, B. and Oraee, K., "Analytical model determining the optimal block size in the block caving mining method", *Indian Geotechnical Journal*, Vol. 45, No. 2, (2015), 156-168. <https://doi.org/10.1007/s40098-014-0119-1>
28. Gao, F., Stead, D. and Coggan, J., "Evaluation of coal longwall caving characteristics using an innovative udec trigon approach", *Computers and Geotechnics*, Vol. 55, No., (2014), 448-460.
29. Song, Z. and Konietzky, H., "A particle-based numerical investigation on longwall top coal caving mining", *Arabian Journal of Geosciences*, Vol. 12, No. 18, (2019), 1-18. <https://doi.org/10.1007/s12517-019-4743-z>
30. Mohammadi, S., Ataei, M., Kakaie, R., Mirzaghobanali, A. and Aziz, N., "A probabilistic model to determine main caving span by evaluating cavability of immediate roof strata in longwall mining", *Geotechnical and Geological Engineering*, Vol. 39, No. 3, (2021), 2221-2237. <https://doi.org/10.1007/s10706-020-01620-y>
31. Wang, J., Wei, W., Zhang, J., Mishra, B. and Li, A., "Numerical investigation on the caving mechanism with different standard deviations of top coal block size in ltcc", *International Journal of Mining Science and Technology*, Vol. 30, No. 5, (2020), 583-591. <https://doi.org/10.1016/j.ijmst.2020.06.001>
32. Alipenhani, B., Majdi, A. and Bakhshandeh Amnieh, H., "Determination of caving hydraulic radius of rock mass in block caving method using numerical modeling and multivariate regression", *Journal of Mining and Environment*, Vol. 13, No. 1, (2022), 217-233. doi: 10.22044/jme.2022.11589.2149.
33. Alipenhani, B., Majdi, A. and Bakhshandeh Amnieh, H., "Cavability assessment of rock mass in block caving mining method based on numerical simulation and response surface methodology", *Journal of Mining and Environment*, Vol. 2, (2022), 579-606. <https://doi.org/10.22044/jme.2022.11858.2176>
34. Jacobsz, S., Kearsley, E., Cumming-Potvin, D. and Wesseloo, J., *Modelling cave mining in the geotechnical centrifuge*, in *Physical modelling in geotechnics*. 2018, CRC Press.809-814.
35. Bai, Q., Tu, S. and Wang, F., "Characterizing the top coal cavability with hard stone band (s): Insights from laboratory physical modeling", *Rock Mechanics and Rock Engineering*, Vol. 52, No. 5, (2019), 1505-1521. <https://doi.org/10.1007/s00603-018-1578-y>
36. Heydarnoori, V., Khosravi, M.H. and Bahaaddini, M., "Physical modelling of caving propagation process and damage profile ahead of the cave-back", *Journal of Mining and Environment*, Vol. 11, No. 4, (2020), 1047-1058. doi: 10.22044/jme.2020.9845.1908.
37. Alipenhani, B., Bakhshandeh Amnieh, H. and Majdi, A., "Physical model simulation of block caving in jointed rock mass", *International Journal of Mining and Geo-Engineering*, (2022). doi: 10.22059/IJMG.2022.339663.594953.
38. Rafiee, R., Ataei, M., Khalokakaie, R., Jalali, S.M.E. and Sereshki, F., "Determination and assessment of parameters influencing rock mass cavability in block caving mines using the probabilistic rock engineering system", *Rock Mechanics and Rock Engineering*, Vol. 48, No. 3, (2015), 1207-1220. <https://doi.org/10.1007/s00603-014-0614-9>

Persian Abstract

چکیده

تعیین ارتفاع تخریب در روش تخریب بلوکی مستلزم در نظر گرفتن معیار مناسب به عنوان معیار تخریب است که در این تحقیق به آن پرداخته شده است. مقایسه معیارهای مختلف تخریب و انتخاب معیار تخریب مناسب برای استفاده در مطالعه قابلیت تخریب توده سنگ ایده اصلی این تحقیق است که در مطالعات قبلی مورد بررسی قرار نگرفته است. در این مقاله با استفاده از نرم افزار اجزاء محدود ارتفاع ناحیه تخریب در مراحل مختلف زیربرش با استفاده از معیارهای جابه‌جایی و شکست برشی و کششی محاسبه شد. نتایج نشان داد که هنگام استفاده از معیار شکست برشی و کششی، ارتفاع تخریب تقریباً ۴ برابر بیشتر از معیار جابه‌جایی است. ارتفاع تخریب در این مورد به ۲۴۹.۱۵ متر می‌رسد. اما این مقدار بر اساس معیارهای جابه‌جایی و کرنش مجاز به ترتیب ۵۹ و ۱۰۷ متر است. طبق روش‌های تجربی، تخریب تا بالاترین ارتفاع بلوک ماده معدنی گسترش می‌یابد. بنابراین، معیار شکست برشی و کششی، ارتفاع تخریب را بهتر از معیار جابه‌جایی پیش‌بینی می‌کند.
